

Correction to the Euler Lagrange multirotor model with Euler angles generalized coordinates

Original

Correction to the Euler Lagrange multirotor model with Euler angles generalized coordinates / Martini, Simone; Valavanis, Kimon P.; Stefanovic, Margareta; Rutherford, Matthew J.; Rizzo, Alessandro. - In: JOURNAL OF INTELLIGENT & ROBOTIC SYSTEMS. - ISSN 0921-0296. - STAMPA. - 110:1(2024). [10.1007/s10846-023-02040-9]

Availability:

This version is available at: 11583/2985384 since: 2024-01-25T14:17:17Z

Publisher:

Springer

Published

DOI:10.1007/s10846-023-02040-9

Terms of use:

This article is made available under terms and conditions as specified in the corresponding bibliographic description in the repository

Publisher copyright

(Article begins on next page)



Correction to the Euler Lagrange Multirotor Model with Euler Angles Generalized Coordinates

Simone Martini¹ · Kimon P. Valavanis¹ · Margareta Stefanovic¹ · Matthew J. Rutherford² · Alessandro Rizzo³

Received: 21 November 2023 / Accepted: 12 December 2023
© The Author(s) 2024

Abstract

This technical note proves analytically how the exact equivalence of the Newton-Euler and Euler-Lagrange modeling formulations as applied to multirotor UAVs is achieved. This is done by deriving a correct Euler-Lagrange multirotor attitude dynamics model. A review of the published literature reveals that the commonly adopted Euler-Lagrange multirotor dynamics model is equivalent to the Newton-Euler model only when it comes to the position dynamics, but not in the attitude dynamics. Step-by-step derivations and calculations are provided to show how modeling equivalence to the Newton-Euler formulation is proven. The modeling equivalence is then verified by obtaining identical results in numerical simulation studies. Simulation results also illustrate that when using the correct model for feedback linearization, controller stability at high gains is improved.

Keywords Multirotor · Modeling · Control

1 Introduction

Derivation of an accurate mathematical model is essential and prerequisite to model-based control of complex dynamic systems in general, and of multirotor UAVs in particular. For example, when considering dynamic inversion control, an accurate mathematical model of the system under consid-

eration should allow for compensation of (any) nonlinear effects, and for linearization of the system dynamics. However, as it happens in almost all cases, it is not realistic to expect complete ‘capture’ of all nonlinear system dynamics effects through a mathematical model, even though the derived model itself does contribute to achieving desirable performance.

When focusing on multirotor UAVs, the Newton-Euler (N-E) and Euler-Lagrange (E-L) formulations are the two main modeling approaches, albeit following different principles; that is, balancing of forces, and the principle of least action, respectively. Regardless, the N-E and E-L formulations are equivalent, and when applied and implemented on multirotor UAVs, they should return identical results.

However, after a thorough literature review, this work reveals that when it comes to the published E-L formulations, when substituting the transformation matrix from the body-fixed frame angular velocity to Euler angle derivatives, the N-E and E-L attitude models are not equivalent - this is shown in detail in Section 3. Hence, the motivation and main objective of this paper is twofold: First, derive a correct E-L (c-E-L) attitude dynamics model for multirotors, registering at the same time the main differences with the E-L formulations used in literature. The proposed c-E-L model is based on the one presented in [1]. Second, prove analytically the

✉ Simone Martini
Simone.Martini@du.edu

✉ Kimon P. Valavanis
Kimon.Valavanis@du.edu

Margareta Stefanovic
Margareta.Stefanovic@du.edu

Matthew J. Rutherford
Matthew.Rutherford@du.edu

Alessandro Rizzo
Alessandro.Rizzo@polito.it

¹ ECE Department, D. F. Ritchie School of Engineering and Computer Science, University of Denver, Denver 80210, CO, USA

² CS Department, D. F. Ritchie School of Engineering and Computer Science, University of Denver, Denver 80210, CO, USA

³ DET, Politecnico di Torino, Torino, Italy

c-E-L model’s equivalence to the N-E formulation (position and attitude dynamics). Then, to show the implementation improvements with the adoption of the c-E-L, the modeling equivalence is demonstrated through numerical simulations on quadrotors.

The quadrotor is studied because it is the most widely used configuration of a multirotor UAV. Its mathematical model description may be found in [2–4], where both formulations are detailed. To be specific, the first E-L formulations may be found in [5–10], while details of the N-E formulation are presented in [11, 12]. Both formulations have been widely used and have been implemented for model-based control and navigation.

State of the art E-L quadrotor models with global validity [13–15] are not affected by the findings in this paper due to the coordinate-free nature of their formulations. Nevertheless, the Euler angle variant of the E-L quadrotor model is still adopted in literature work [16, 17], which supports further the correction proposed in this paper. The findings of this work are coherent to the general attitude E-L formulation of [18], which was published at the time of writing this paper. Although following different approaches, both papers arrive, independently, at the same result.

The rest of the paper is organized as follows. Section 2 introduces the required notation, and the N-E and E-L quadrotor dynamics models as found in the related literature. Section 3 details the proposed c-E-L model and proves its equivalence to the existing N-E model found in the literature. Section 4 includes simulation results. Controller performance comparisons between the proposed and existing models verify and illustrate the equivalence between the two modeling approaches as presented in this paper. Lastly, in Section 5, conclusions are offered.

2 Notation and Background Information

2.1 Notation

Let I_n denote the $n \times n$ identity matrix. Moreover, given vectors $a, b \in \mathbb{R}^3$, denote $S(a)b = a \times b$, where

$$S(a) = \begin{bmatrix} 0 & -a_3 & a_2 \\ a_3 & 0 & -a_1 \\ -a_2 & a_1 & 0 \end{bmatrix} \tag{1}$$

is the 3×3 skew symmetric matrix composed of the elements of a . In addition, consider the unit vector $\mathbf{e}_3 = [0, 0, 1]^T$. The notation $\frac{da}{dt}$ and \dot{a} is used interchangeably throughout the paper.

In what follows, for clarity purposes, the N-E and E-L quadrotor dynamics are considered, which may be easily generalized to any multirotor UAV dynamics.

2.2 Quadrotor Nonlinear Dynamics

The N-E quadrotor dynamics, as presented in [2], are described by the following equations

$$J\dot{\omega} = M - S(\omega)J\omega, \tag{2}$$

$$\dot{v} = \frac{1}{m}T\mathbf{e}_3 - S(\omega)v - gR^T(\eta)\mathbf{e}_3, \tag{3}$$

where $S(\omega) \in \mathbb{R}^{3 \times 3}$ is the skew symmetric matrix of the angular velocities, ω , defined in the body-fixed frame, $J \in \mathbb{R}^{3 \times 3}$ is the constant diagonal inertia matrix, M is the external torque induced by the quadrotor propellers in the body-fixed frame, v is the quadrotor linear velocity vector in the body-fixed reference frame, m is the total mass of the quadrotor, g is the gravitational acceleration, and T is the total produced thrust. The matrix $R(\eta) \in \mathbb{R}^{3 \times 3}$ represents the rotation from the body-fixed frame to the inertial frame. Note that the choice of $R(\eta)$ is not unique since the quadrotor dynamics are invariant to any choice of Euler angles configuration that may be used to represent the attitude of the quadrotor.

The E-L formulation, as introduced in [19], is represented by the following two equations

$$\ddot{\eta} = J_R^{-1}(\eta)(M - C(\eta, \dot{\eta})\dot{\eta}), \tag{4}$$

$$\ddot{p} = \frac{1}{m}TR(\eta)\mathbf{e}_3 - g\mathbf{e}_3, \tag{5}$$

where $\eta = [\phi, \theta, \psi]^T$ is the vector of any choice of Euler angles configuration, and $p = [x, y, z]^T$ is the inertial reference frame position vector. $J_R(\eta)$ is the rotated inertia matrix and $C(\eta, \dot{\eta})$ is the matrix accounting for centrifugal and Coriolis effects.

3 Equivalence of the N-E and E-L Modeling Formulations

To verify if the E-L and N-E models are equivalent, a coordinate transformation should lead from one formulation to the other. Starting from the position dynamics, the linear velocity expressed in the body-fixed frame is related to the inertial frame velocity by the following equation

$$v = R^T(\eta)\dot{p} \tag{6}$$

Thus, by substituting Eqs. 6 in 3, the following equation is derived (with all steps shown in detail)

$$\frac{d(R^T(\eta)\dot{p})}{dt} = -S(\omega)R^T(\eta)\dot{p} - gR^T(\eta)\mathbf{e}_3 + \frac{1}{m}T\mathbf{e}_3$$

$$\begin{aligned}
 R^T(\eta)\dot{p} + R^T(\eta)\ddot{p} &= -S(\omega)R^T(\eta)\dot{p} - gR^T(\eta)\mathbf{e}_3 + \frac{1}{m}T\mathbf{e}_3 \\
 \underline{S(\omega)^T R^T(\eta)\dot{p}} + R^T(\eta)\ddot{p} &= \underline{-S(\omega)R^T(\eta)\dot{p}} - gR^T(\eta)\mathbf{e}_3 + \frac{1}{m}T\mathbf{e}_3 \\
 \ddot{p} &= -g\mathbf{e}_3 + \frac{1}{m}TR(\eta)\mathbf{e}_3 \tag{7}
 \end{aligned}$$

The resulting equation is the same as Eq. 5, thus, the equivalence between the N-E and E-L position dynamics formulations (as found in the literature) is proven.

However, the relationship between the Euler angles derivatives $\dot{\eta}$ and the angular velocities ω is less intuitive. This relationship may be derived by considering the rotation from the inertial reference frame (IF) to the body-fixed frame (BF) as the composition of three elementary rotations. To achieve this, two intermediate reference frames are defined, F1 and F2, respectively. Following [20], without loss of generality, to show how this relationship is derived, the Tait-Bryan 321 sequence of rotations is employed as shown in Fig. 1, and it is detailed next.

• IF → F1

F1 is obtained from the elementary rotation of an angle ψ with respect to the z -axis of the IF, defined as $R_3(\psi)^T = R_3(-\psi)$. The related angular velocity in the IF is $\omega_{\psi,I} = [0, 0, \dot{\psi}]^T$. It follows that the angular velocity in F1 is given by $\omega_{\psi,1} = R_3(-\psi)\omega_{\psi,I} = \omega_{\psi,I}$.

• F1 → F2

F2 is obtained from the elementary rotation of an angle θ with respect to the y_1 -axis of F1, defined as $R_2(\theta)^T = R_2(-\theta)$. The related angular velocity in F1 is $\omega_{\theta,1} = [0, \dot{\theta}, 0]^T$. It follows that the angular velocity in F2 is given by $\omega_{\theta,2} = R_2(-\theta)\omega_{\theta,1} = \omega_{\theta,1}$. Moreover, in F2, the angular velocity related to the angle ψ is $\omega_{\psi,2} = R_2(-\theta)\omega_{\psi,1} = R_2(-\theta)\omega_{\psi,I}$.

• F2 → BF

BF is obtained from the elementary rotation of an angle ϕ with respect to the x_2 -axis of F2, defined as $R_1(\phi)^T = R_1(-\phi)$. The related angular velocity in F2 is $\omega_{\phi,2} =$

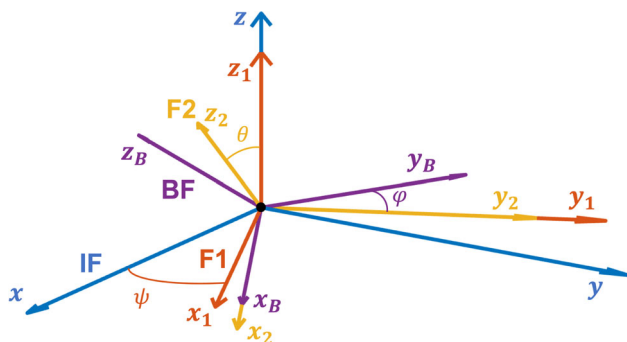


Fig. 1 Tait-Bryan 321 Sequence of Elementary Rotations from IF to BF

$[\dot{\phi}, 0, 0]^T$. It follows that the angular velocity in BF is given by $\omega_{\phi,B} = R_1(-\phi)\omega_{\phi,2} = \omega_{\phi,2}$. Moreover, in BF, the angular velocity related to the angle θ is $\omega_{\theta,B} = R_1(-\phi)\omega_{\theta,2} = R_1(-\phi)\omega_{\theta,1}$. Finally, in BF, the angular velocity related to the angle ψ is $\omega_{\psi,B} = R_1(-\phi)\omega_{\psi,2} = R_1(-\phi)R_2(-\theta)\omega_{\psi,I}$.

Therefore, the angular velocity as expressed in the BF is

$$\begin{aligned}
 \omega &= \omega_{\phi,B} + \omega_{\theta,B} + \omega_{\psi,B} = \omega_{\phi,2} + R_1(-\phi)\omega_{\theta,1} \\
 &\quad + R_1(-\phi)R_2(-\theta)\omega_{\psi,I} = \\
 &= \begin{bmatrix} \dot{\phi} \\ 0 \\ 0 \end{bmatrix} + R_1(-\phi) \begin{bmatrix} 0 \\ \dot{\theta} \\ 0 \end{bmatrix} + R_1(-\phi)R_2(-\theta) \begin{bmatrix} 0 \\ 0 \\ \dot{\psi} \end{bmatrix} = \\
 &= I_{31}\dot{\phi} + A_2\dot{\theta} + B_3\dot{\psi} = \underbrace{[I_{31}, A_2, B_3]}_{=W(\eta)} \begin{bmatrix} \dot{\phi} \\ \dot{\theta} \\ \dot{\psi} \end{bmatrix} \tag{8}
 \end{aligned}$$

where I_{31} is the first column of the 3×3 identity matrix, A_2 is the second column of $A = R_1(-\phi)$, and B_3 is the third column of $B = R_1(-\phi)R_2(-\theta)$.

Thus, in more compact form

$$\omega = W(\eta)\dot{\eta} \tag{9}$$

$$\dot{\eta} = W^{-1}(\eta)\omega \tag{10}$$

where W depends on the choice of the Euler angle sequence. One example, for clarification purposes, may be found in [21]. Kinematic relations Eqs. 9 and 10 are invariant to the choice of the Euler angles, but the configuration needs to be consistent with the choice of R . However, different Euler angles configurations will result in a different W , and so, given Eq. 10, it is recommended to choose a configuration in which W is invertible for the whole flight envelope, see [19], except when the pitch angle is equal to π (an uncommon state outside acrobatic manoeuvres).

When substituting Eq. 9 in the N-E attitude model Eq. 2, this leads to

$$\begin{aligned}
 M &= \frac{d(J(W(\eta)\dot{\eta}))}{dt} + S(W(\eta)\dot{\eta})JW(\eta)\dot{\eta} \\
 M &= J\dot{W}(\eta)\dot{\eta} + JW(\eta)\ddot{\eta} + S(W(\eta)\dot{\eta})JW(\eta)\dot{\eta} \\
 M &= JW(\eta)\ddot{\eta} + (J\dot{W}(\eta) + S(W(\eta)\dot{\eta})JW(\eta))\dot{\eta}
 \end{aligned} \tag{11}$$

where $S(W\dot{\eta})$ is the skew symmetric matrix of $W(\eta)\dot{\eta}$.

When compared to the literature E-L model shown in Eq. 4, which can be rewritten as

$$M = J_R(\eta)\ddot{\eta} + C(\eta, \dot{\eta})\dot{\eta} \tag{12}$$

it leads to the following inequalities

$$J_R(\eta)\ddot{\eta} = W^T(\eta)JW(\eta)\ddot{\eta} \neq JW(\eta)\ddot{\eta} \tag{13}$$

$$C(\eta, \dot{\eta})\dot{\eta} = \left(J_R - \frac{1}{2} \frac{\partial(\dot{\eta}^T J_R)}{\partial \eta} \right) \dot{\eta} \neq (J\dot{W}(\eta) + S(W(\eta)\dot{\eta})JW(\eta)) \dot{\eta} \tag{14}$$

and, in general, contrary to what should be expected, the multirotor attitude dynamics following the E-L and N-E formulations found in the literature do not produce an equivalent result given that

$$J\dot{\omega} - S(\omega)J\omega \neq J_R(\eta)\ddot{\eta} + C(\eta, \dot{\eta})\dot{\eta} \tag{15}$$

However, this shortcoming may be rectified based on the approach introduced in [1], in which a proof is provided for the equivalence of the projective N-E equations and the E-L equations of second kind for spatial rigid multibody systems. Considering the proof in [1], it is shown that for multirotor UAVs (including quadrotors), the attitude dynamics E-L equations should be written in the following form

$$\frac{d}{dt} \frac{\partial L}{\partial \dot{\eta}} - \frac{\partial L}{\partial \eta} = W^T(\eta)M \tag{16}$$

instead of the one presented in [2], that is

$$\frac{d}{dt} \frac{\partial L}{\partial \dot{\eta}} - \frac{\partial L}{\partial \eta} = M \tag{17}$$

with the Lagrangian, $L = \frac{1}{2}\omega^T J\omega$, which, in the case of attitude dynamics, is equivalent to the rotational kinetic energy.

An intuitive reason for writing the c-E-L form as Eq. 16 is given by noticing that a premultiplication of W^T would result in Eqs. 13 and 14 being equalities. Moreover, this approach is similar to the quaternion variant of the E-L formulation as shown in [22]. Building on the above observation, it is now shown that the same steps presented in [1] may be followed to model multirotor UAVs / quadrotors.

Since it is considered that the forces are applied to the center of mass of the quadrotor (multirotor), the position and attitude dynamics can be analyzed independently. Hence, only the E-L equations for the angular dynamics are derived.

To prove the equivalence of the c-E-L model, to the N-E model, the following relations are defined first. For better readability, W is written without explicit dependence on η .

Relation 1 Consider $W(\eta)^{-1}$, the rows of which are given by $w_{inv,1}, w_{inv,2}, w_{inv,3}$, as follows

$$W^{-1} = \begin{pmatrix} w_{inv,1} \\ w_{inv,2} \\ w_{inv,3} \end{pmatrix} \tag{18}$$

Next, define the matrix

$$\Sigma(W^{-1}) = \begin{pmatrix} \frac{\partial w_{inv,1}^T}{\partial \eta} W^{-1} \\ \frac{\partial w_{inv,2}^T}{\partial \eta} W^{-1} \\ \frac{\partial w_{inv,3}^T}{\partial \eta} W^{-1} \end{pmatrix} - \begin{pmatrix} (\frac{\partial w_{inv,1}^T}{\partial \eta} W^{-1})^T \\ (\frac{\partial w_{inv,2}^T}{\partial \eta} W^{-1})^T \\ (\frac{\partial w_{inv,3}^T}{\partial \eta} W^{-1})^T \end{pmatrix} = \begin{pmatrix} S(w_{inv,1}) \\ S(w_{inv,2}) \\ S(w_{inv,3}) \end{pmatrix} \tag{19}$$

This matrix, for any Euler angle sequence, is composed of the skew symmetric matrices of $S(w_{inv,i})$ with $i = 1, 2, 3$.

Relation 2 Note that the time derivative of W^{-1} can be expressed as

$$\frac{dW^{-1}}{dt} = \begin{pmatrix} \frac{\partial w_{inv,1}^T}{\partial \eta} \dot{\eta} \\ \frac{\partial w_{inv,2}^T}{\partial \eta} \dot{\eta} \\ \frac{\partial w_{inv,3}^T}{\partial \eta} \dot{\eta} \end{pmatrix} = \begin{pmatrix} \dot{\eta}^T (\frac{\partial w_{inv,1}^T}{\partial \eta})^T \\ \dot{\eta}^T (\frac{\partial w_{inv,2}^T}{\partial \eta})^T \\ \dot{\eta}^T (\frac{\partial w_{inv,3}^T}{\partial \eta})^T \end{pmatrix} = \begin{pmatrix} \omega^T (\frac{\partial w_{inv,1}^T}{\partial \eta} W^{-1})^T \\ \omega^T (\frac{\partial w_{inv,2}^T}{\partial \eta} W^{-1})^T \\ \omega^T (\frac{\partial w_{inv,3}^T}{\partial \eta} W^{-1})^T \end{pmatrix} \tag{20}$$

Relation 3 The following is obvious

$$\frac{\partial \eta}{\partial \eta} = \frac{\partial \dot{\eta}}{\partial \dot{\eta}} = \frac{\partial(W^{-1}\omega)}{\partial \dot{\eta}} = W^{-1} \frac{\partial \omega}{\partial \dot{\eta}} = I \tag{21}$$

Relation 4 From Relation 3, the following holds

$$\frac{\partial W^{-1}}{\partial \eta} \omega = \begin{pmatrix} \omega^T (\frac{\partial w_{inv,1}^T}{\partial \eta}) \\ \omega^T (\frac{\partial w_{inv,2}^T}{\partial \eta}) \\ \omega^T (\frac{\partial w_{inv,3}^T}{\partial \eta}) \end{pmatrix} = \begin{pmatrix} \omega^T (\frac{\partial w_{inv,1}^T}{\partial \eta}) W^{-1} \\ \omega^T (\frac{\partial w_{inv,2}^T}{\partial \eta}) W^{-1} \\ \omega^T (\frac{\partial w_{inv,3}^T}{\partial \eta}) W^{-1} \end{pmatrix} \frac{\partial \omega}{\partial \dot{\eta}} \tag{22}$$

Relation 5 In addition, using Relation 3, it is true that

$$\left(\frac{\partial W^{-1}\omega}{\partial \eta} \right) = \frac{\partial \dot{\eta}}{\partial \eta} = \frac{d}{dt} \left(\frac{\partial \eta}{\partial \eta} \right) = \frac{d}{dt} \left(W^{-1} \frac{\partial \omega}{\partial \dot{\eta}} \right) \tag{23}$$

that leads to the following

$$\left(\frac{\partial W^{-1}\omega}{\partial \eta} \right) = \frac{d}{dt} (W^{-1}) \frac{\partial \omega}{\partial \dot{\eta}} + W^{-1} \frac{d}{dt} \left(\frac{\partial \omega}{\partial \dot{\eta}} \right) \tag{24}$$

Relation 6 Rearranging Relation 5 and substituting Eqs. 20, 22, and 19, the following equality is obtained

$$\begin{aligned} \frac{d}{dt} \left(\frac{\partial \omega}{\partial \dot{\eta}} \right) &= W \left(\frac{\partial W^{-1} \omega}{\partial \eta} - \frac{d}{dt} (W^{-1}) \frac{\partial \omega}{\partial \dot{\eta}} \right) = \\ &= W \left(W^{-1} \frac{\partial \omega}{\partial \eta} + \frac{\partial W^{-1}}{\partial \dot{\eta}} \omega - \frac{d}{dt} (W^{-1}) \frac{\partial \omega}{\partial \dot{\eta}} \right) = \\ &= \frac{\partial \omega}{\partial \eta} + W \left[\begin{array}{l} \omega^T \left(\frac{\partial w_{inv,1}^T}{\partial \eta} \right) W^{-1} \\ \omega^T \left(\frac{\partial w_{inv,2}^T}{\partial \eta} \right) W^{-1} \\ \omega^T \left(\frac{\partial w_{inv,3}^T}{\partial \eta} \right) W^{-1} \end{array} \right] \\ &\quad - \left[\begin{array}{l} \omega^T \left(\frac{\partial w_{inv,1}^T}{\partial \eta} W^{-1} \right)^T \\ \omega^T \left(\frac{\partial w_{inv,2}^T}{\partial \eta} W^{-1} \right)^T \\ \omega^T \left(\frac{\partial w_{inv,3}^T}{\partial \eta} W^{-1} \right)^T \end{array} \right] \frac{\partial \omega}{\partial \dot{\eta}} = \\ &= \frac{\partial \omega}{\partial \eta} + W \left(\begin{array}{l} \omega^T S(w_{inv,1}) \\ \omega^T S(w_{inv,2}) \\ \omega^T S(w_{inv,3}) \end{array} \right) \frac{\partial \omega}{\partial \dot{\eta}} = \\ &= \frac{\partial \omega}{\partial \eta} + W \left(\begin{array}{l} -w_{inv,1} S(\omega) \\ -w_{inv,2} S(\omega) \\ -w_{inv,3} S(\omega) \end{array} \right) \frac{\partial \omega}{\partial \dot{\eta}} = \\ &= \frac{\partial \omega}{\partial \eta} - \underbrace{W W^{-1}}_{=I_3} S(\omega) \frac{\partial \omega}{\partial \dot{\eta}} \end{aligned} \tag{25}$$

leading to

$$\frac{d}{dt} \left(\frac{\partial \omega}{\partial \dot{\eta}} \right) = \frac{\partial \omega}{\partial \eta} - S(\omega) \frac{\partial \omega}{\partial \dot{\eta}} \tag{26}$$

Relation 7 Considering Eq. 9 it is easy to show that

$$\left(\frac{\partial \omega}{\partial \dot{\eta}} \right)^T = \frac{(\partial \dot{\eta}^T W^T)}{\partial \dot{\eta}} = W^T \tag{27}$$

Given the relationships above, it is shown next that the c-E-L formulation leads to an equivalent result with the N-E attitude model.

Proof The multirotor c-E-L formulation Eq. 16 can be rewritten as

$$\frac{d}{dt} \left(\frac{\partial \frac{1}{2} \omega^T J \omega}{\partial \dot{\eta}} \right) - \frac{\partial \frac{1}{2} \omega^T J \omega}{\partial \eta} = W^T M \tag{28}$$

Since J is a constant symmetric matrix, this is equivalent to

$$\begin{aligned} \frac{d}{dt} \left[\left(\frac{\partial \omega}{\partial \dot{\eta}} \right)^T J \omega \right] - \left(\frac{\partial \omega}{\partial \eta} \right)^T J \omega &= W^T M \\ \frac{d}{dt} \left[\left(\frac{\partial \omega}{\partial \dot{\eta}} \right)^T \right] J \omega + \left(\frac{\partial \omega}{\partial \dot{\eta}} \right)^T J \dot{\omega} - \left(\frac{\partial \omega}{\partial \eta} \right)^T J \omega &= W^T M \end{aligned} \tag{29}$$

From Eq. 29, by using Relations 6 and 7 one obtains

$$\begin{aligned} \left[\left(\frac{\partial \omega}{\partial \dot{\eta}} \right)^T + \left(\frac{\partial \omega}{\partial \dot{\eta}} \right)^T S(\omega) \right] J \omega + \left(\frac{\partial \omega}{\partial \dot{\eta}} \right)^T J \dot{\omega} - \left(\frac{\partial \omega}{\partial \eta} \right)^T J \omega &= W^T M \\ W^T S(\omega) J \omega + W^T J \dot{\omega} &= W^T M \end{aligned} \tag{30}$$

And, for W having full rank, Eq. 30 is rewritten as

$$J \dot{\omega} + S(\omega) J \omega = M \tag{31}$$

This corresponds to the N-E quadrotor model formulation. This equivalence does not hold when using the E-L formulation from the literature Eq. 17. This concludes the proof.

Therefore, the proposed attitude c-E-L model is

$$W^T M = J_R \ddot{\eta} + C \dot{\eta} \tag{32}$$

which rectifies the literature E-L model of Eq. 12 and this result reconfirms and agrees with findings in [18] for the general attitude dynamics.

4 Comparison with Previous Formulations

Given the proof of the mathematical equivalence of the c-E-L and N-E, it is straightforward to state that the presented formulation leads to improved performance with respect to the E-L quadrotor model found in literature. This section shows the difference in performance considering the model employed in Sections 4.1 and 4.2, as simulation platform, and in Section 4.3, for model-based control.

4.1 Implementation Comparison Between the Different Models

In this section, it is shown that the error between the c-E-L and N-E formulations is lower compared to the one between the E-L and N-E formulations. To do so, the same rotor input velocity, $u = [475.9 + 0.1 \sin t, 476.2 + 0.1 \sin t, 476, 476.1]$ is applied to the (N-E, E-L, c-E-L) quadrotor models for a period of 60s, and the root mean square error (RMSE) is computed for the generalized coordinates ($p, \eta, \dot{p}, \dot{\eta}$). The choice of these rotor inputs is such that the quadrotor will cover a long range in x, y, z , while having non constant attitude and not reaching any singular configuration. From Table 1, which illustrates results with an integration step of 10ms, it is evident that the c-E-L has a RMSE of 3 to 6 orders of magnitude smaller than the literature E-L.

Table 1 Comparison with E-L model from literature (10ms)

	E-L	c-E-L
$RMSE_p$	1.853	67.976×10^{-6}
$RMSE_\eta$	8.135×10^{-3}	496.720×10^{-9}
$RMSE_{\dot{p}}$	160.833×10^{-3}	6.210×10^{-6}
$RMSE_{\dot{\eta}}$	4.416×10^{-3}	21.692×10^{-9}

Moreover, Table 2 shows that by further decreasing the integration step to $1ms$, the error of the correct model decreases even more, while this is not true for the E-L model found in literature E-L, leading to an error of 6 to 9 order of magnitude smaller.

Note that, even though they are studied independently, the position dynamics are affected by the attitude dynamics due to the influence of the rotation matrix. For this reason it is worth considering the RMSE for p and \dot{p} as well.

4.2 Comparison with Multibody Dynamic Simulator

Now, the comparison of these mathematical models with respect to a multibody dynamic simulator such as Mathworks's Simscape Multibody is considered. Note that Simscape Multibody uses its own dynamic engine to solve the equation of motions, while only the structure and the inertia of the quadrotor is provided by the user. As shown in Table 3, providing the same input as before to all models, the N-E and the c-E-L state dynamics are almost identical to the one of a multibody dynamic simulator, while the literature E-L model has a much larger error. Again, as shown in Table 4, this becomes even more evident when decreasing the simulation step to $1ms$.

It is essential to state that in order to achieve these error magnitudes, all mathematical models (N-E, E-L, c-E-L) need to account for the gyroscopic effect, which is automatically computed in the dynamic simulator. The gyroscopic effect is modeled as in [19], and since it depends on the external input u , for the c-E-L model, it is pre multiplied by W^T .

Table 2 Comparison with E-L model from literature (1ms)

	E-L	c-E-L
$RMSE_p$	1.853	68.297×10^{-9}
$RMSE_\eta$	8.135×10^{-3}	499.466×10^{-12}
$RMSE_{\dot{p}}$	160.828×10^{-3}	6.240×10^{-9}
$RMSE_{\dot{\eta}}$	4.436×10^{-3}	21.821×10^{-12}

Table 3 Comparison with multibody dynamic simulator (10ms)

	N-E	E-L	c-E-L
$RMSE_p$	130.785×10^{-6}	1.853	149.865×10^{-6}
$RMSE_\eta$	255.423×10^{-6}	8.338×10^{-3}	255.868×10^{-6}
$RMSE_{\dot{p}}$	6.535×10^{-6}	160.833×10^{-3}	9.841×10^{-6}
$RMSE_{\dot{\eta}}$	461.558×10^{-6}	4.354×10^{-3}	461.559×10^{-6}

4.3 Effect on Model Based Control

By implementing a PID controller with feedback linearization on the multibody dynamic simulator quadrotor the different effects of the E-L and c-E-L are analyzed. The helix trajectory to track is displayed in Fig. 2, along the resulting in the attitude trajectory.

The attitude errors resulting from the numerical simulations with different PID gain configurations are shown in Fig. 3. While at some gain values the controller performance is identical, it is shown that by increasing the controller gains, the controller that uses the c-E-L for dynamic compensation has bigger margin of stability. The feedback linearization using the literature E-L model leads to unstable behaviour with smaller gain compared to the c-E-L.

5 Conclusions

A correct E-L attitude dynamics model of quadrotors / multirotor UAVs has been presented and derived. The equivalence to the N-E formulation has been demonstrated through analytical steps and numerical simulations. Compared to existing E-L formulations found in literature, the c-E-L model is equivalent to the N-E model and therefore, when exploited for dynamic compensation, it provides better stability of the closed loop controlled system. Building on this work, previously presented feedback linearization controllers using E-L formulation (including the ones from the authors) could be improved.

Table 4 Comparison with multibody dynamic simulator (1ms)

	N-E	E-L	c-E-L
$RMSE_p$	130.965×10^{-6}	1.853	130.968×10^{-6}
$RMSE_\eta$	25.550×10^{-6}	8.155×10^{-3}	25.551×10^{-6}
$RMSE_{\dot{p}}$	6.550×10^{-6}	160.828×10^{-3}	6.551×10^{-6}
$RMSE_{\dot{\eta}}$	46.303×10^{-6}	4.429×10^{-3}	46.303×10^{-6}

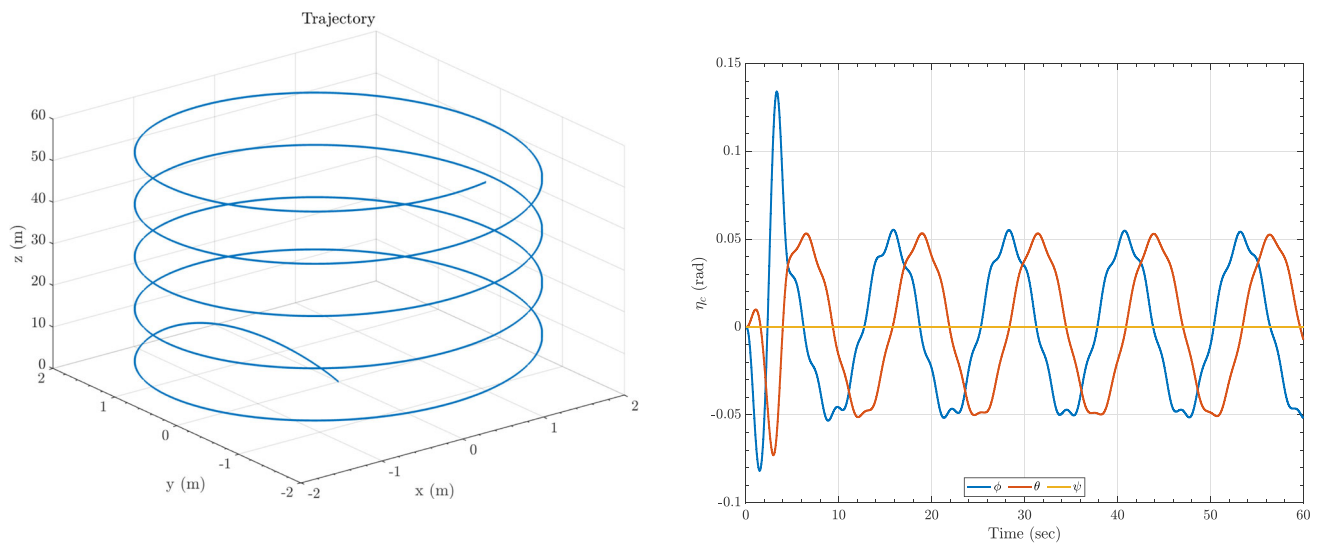
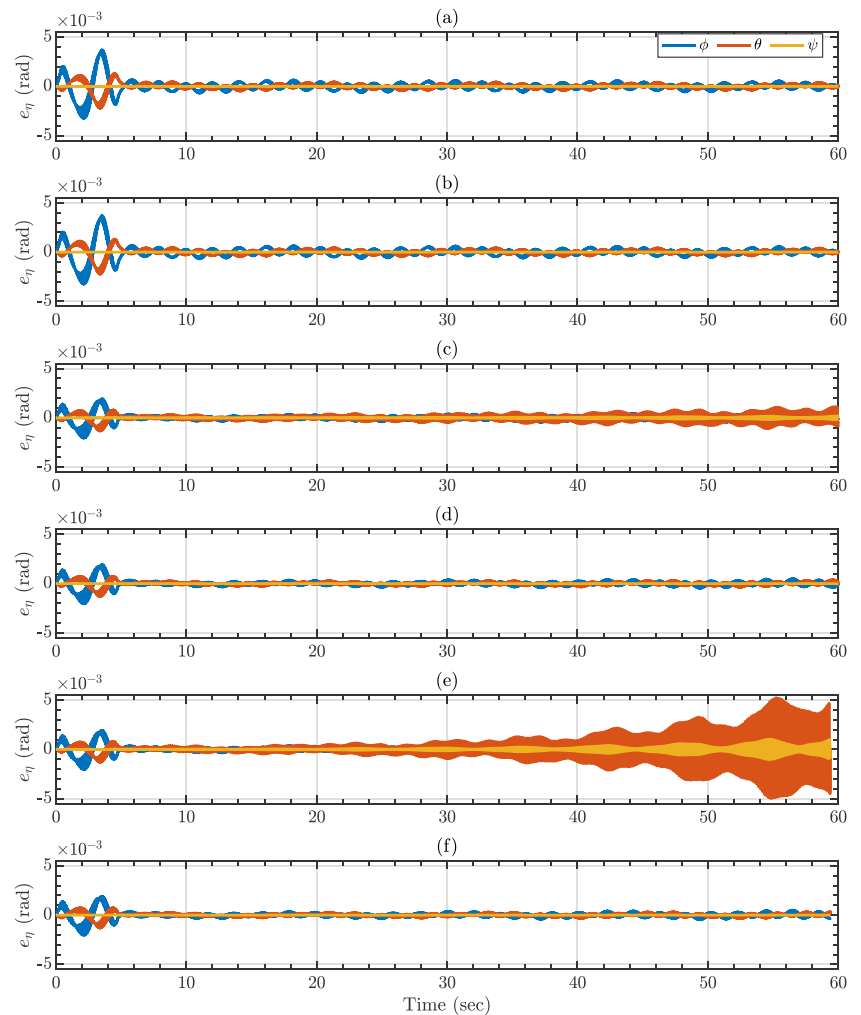


Fig. 2 3D Trajectory (left) & attitude trajectory (right)

Fig. 3 Closed loop system attitude error e_{η} . (a),(c),(e) use literature E-L for dynamic compensation, (b),(d),(f) use c-E-L for dynamic compensation. Controller gain $K_i = 8 \times 10^3, 15.5 \times 10^3, 16 \times 10^3$ respectively



Acknowledgements This work is part of the Ph.D. research of Simone Martini conducted at the University of Denver Unmanned Systems Research Institute (DU²SRI) in collaboration with Politecnico di Torino.

Dr. Rizzo is supported by the MOST - Sustainable Mobility National Research Center and received funding from the European Union Next-GenerationEU (PIANO NAZIONALE DI RIPRESA E RESILIENZA (PNRR) - MISSIONE 4 COMPONENTE 2, INVESTIMENTO 1.4 - D.D. 1033 17/06/2022, CN00000023).

A pre print version of this technical note has been uploaded to <https://doi.org/10.48550/arXiv.2310.09306>.

Author Contributions Simone Martini contributed to the study conception. The study was designed by Simone Martini, Dr. Kimon Valavanis, and Dr. Alessandro Rizzo. Literature Review was written by Simone Martini and Dr. Kimon Valavanis. Mathematical proof was written by Simone Martini under supervision of Dr. Kimon Valavanis and Dr. Margareta Stefanovic. Data analysis was performed by all authors. The first draft of the manuscript was written by Simone Martini and all authors commented on previous versions of the manuscript.

Funding Not applicable

Availability of data and materials Not applicable

Code availability Not applicable

Declarations

Ethics approval Not applicable

Consent to participate Not applicable

Consent for publication Not applicable

Conflicts of interest Not applicable

Open Access This article is licensed under a Creative Commons Attribution 4.0 International License, which permits use, sharing, adaptation, distribution and reproduction in any medium or format, as long as you give appropriate credit to the original author(s) and the source, provide a link to the Creative Commons licence, and indicate if changes were made. The images or other third party material in this article are included in the article's Creative Commons licence, unless indicated otherwise in a credit line to the material. If material is not included in the article's Creative Commons licence and your intended use is not permitted by statutory regulation or exceeds the permitted use, you will need to obtain permission directly from the copyright holder. To view a copy of this licence, visit <http://creativecommons.org/licenses/by/4.0/>.

References

- Gaull, A.: A rigorous proof for the equivalence of the projective newton-euler equations and the lagrange equations of second kind for spatial rigid multibody systems. *Multibody Sys.Dyn.* **45**(1), 87–103 (2019)
- Luukkonen, T.: Modelling and control of quadcopter. Independent research project in applied mathematics. Espoo. **22**(22) (2011)
- Bouabdallah, S.: Design and control of quadrotors with application to autonomous flying. Technical report, Epfl (2007)
- Lee, H., Kim, H.J.: Trajectory tracking control of multirotors from modelling to experiments: a survey. *Int. J. Control Autom. Syst.* **15**, 281–292 (2017)
- Bouabdallah, S., Noth, A., Siegwart, R.: Pid vs lq control techniques applied to an indoor micro quadrotor. In: 2004 IEEE/RSJ International Conference on Intelligent Robots and Systems (IROS)(IEEE Cat. No. 04CH37566), vol. 3, pp. 2451–2456 (2004). IEEE
- Castillo, P., Dzul, A., Lozano, R.: Real-time stabilization and tracking of a four-rotor mini rotorcraft. *IEEE Trans. Control Syst. Technol.* **12**(4), 510–516 (2004)
- Castillo, P., Lozano, R., Dzul, A.: Stabilization of a mini-rotorcraft having four rotors. In: 2004 IEEE/RSJ International Conference on Intelligent Robots and Systems (IROS)(IEEE Cat. No. 04CH37566), vol. 3, pp. 2693–2698 (2004). IEEE
- Raffo, G.V., Ortega, M.G., Rubio, F.R.: Backstepping/nonlinear h ∞ control for path tracking of a quadrotor unmanned aerial vehicle. In: 2008 American Control Conference, pp. 3356–3361 (2008). IEEE
- Raffo, G.V., Ortega, M.G., Rubio, F.R.: An integral predictive/nonlinear h ∞ control structure for a quadrotor helicopter. *Automatica* **46**(1), 29–39 (2010)
- Das, A., Lewis, F., Subbarao, K.: Backstepping approach for controlling a quadrotor using lagrange form dynamics. *J. Intell. Rob. Syst.* **56**, 127–151 (2009)
- Mahony, R., Kumar, V., Corke, P.: Multirotor aerial vehicles: modeling, estimation, and control of quadrotor. *IEEE Robotics & Automation Magazine.* **19**(3), 20–32 (2012). <https://doi.org/10.1109/MRA.2012.2206474>
- L'afflitto, A., Anderson, R.B., Mohammadi, K.: An introduction to nonlinear robust control for unmanned quadrotor aircraft: How to design control algorithms for quadrotors using sliding mode control and adaptive control techniques [focus on education]. *IEEE Control Syst. Mag.* **38**(3), 102–121 (2018)
- Duindam, V., Stramigioli, S.: Singularity-free dynamic equations of open-chain mechanisms with general holonomic and nonholonomic joints. *IEEE Trans. Rob.* **24**(3), 517–526 (2008). <https://doi.org/10.1109/TRO.2008.924250>
- From, P.J.: An explicit formulation of singularity-free dynamic equations of mechanical systems in lagrangian form—part two: multibody systems. (2012)
- Welde, J., Kumar, V.: Coordinate-free dynamics and differential flatness of a class of 6dof aerial manipulators, 4307–4313 (2020). <https://doi.org/10.1109/ICRA40945.2020.9196705>
- Lavín-Delgado, J., Beltrán, Z.Z., Gómez-Aguilar, J., Pérez-Careta, E.: Controlling a quadrotor uav by means of a fractional nested saturation control. *Adv. Space Res.* **71**(9), 3822–3836 (2023)
- Wang, S., Polyakov, A., Zheng, G.: Quadrotor stabilization under time and space constraints using implicit pid controller. *J. Franklin Inst.* **359**(4), 1505–1530 (2022)
- Bernstein, D.S., Goel, A., Kouba, O.: Deriving euler's equation for rigid-body rotation via lagrangian dynamics with generalized coordinates. *Mathematics.* **11**(12), 2727 (2023)
- Martini, S., Sönmez, S., Rizzo, A., Stefanovic, M., Rutherford, M.J., Valavanis, K.P.: Euler-lagrange modeling and control of quadrotor uav with aerodynamic compensation. In: 2022 International Conference on Unmanned Aircraft Systems (ICUAS), pp. 369–377 (2022). IEEE
- Novara, C.: Lecture notes in Attitude Kinematics. Nonlinear Control and Aerospace Applications, Department of Electronics and Telecommunications (DET) (2020)
- Beard, R.: Quadrotor dynamics and control rev 0.1. (2008)
- Alaimo, A., Artale, V., Milazzo, C., Ricciardello, A., Trefiletti, L.: Mathematical modeling and control of a hexacopter. In: 2013 International Conference on Unmanned Aircraft Systems (ICUAS), pp. 1043–1050 (2013). <https://doi.org/10.1109/ICUAS.2013.6564793>

Publisher's Note Springer Nature remains neutral with regard to jurisdictional claims in published maps and institutional affiliations.

Simone Martini is a Ph.D. candidate in the Electrical and Computer Engineering department at the University of Denver, working under the supervision of Dr. Kimon P. Valavanis at University of Denver Unmanned Systems Research Institute (DU²SRI) and Dr. Alessandro Rizzo at Politecnico di Torino. He obtained his B.S. in Aerospace Engineering and M.S. in Mechatronics Engineering from Politecnico di Torino. His research interest revolve around nonlinear modeling and control of UAV.

Kimon P. Valavanis Ph.D., is John Evans Professor, Department of ECE, D. F. Ritchie School of Engineering and Computer Science, University of Denver. He is Guest Professor in the Faculty of Electrical Engineering and Computing, University of Zagreb, Croatia. He also held Visiting Appointments at Politecnico di Torino, Dipartimento di Ingegneria Meccanica e Aerospaziale, DIMEAS, and he was Professeur Invité, Université de Lorraine - Polytech Nancy, in France. His research interests span Unmanned Systems, Distributed Intelligence Systems, Robotics and Automation. He has published more than 450 book chapters, technical journal, and transaction, referred conference, and invited papers. He has authored/co-authored/edited 19 books. He has graduated 40 Ph.D. students and more than 100 M.Sc. students. Dr. Valavanis served as Editor-in-Chief of the Robotics and Automation Magazine from 1996–2005, and since 2006, of the Journal of Intelligent and Robotic Systems, Springer. He also serves as cochair of the Aerial Robotics and Unmanned Aerial Vehicles Technical Committee since 2008. He founded the International Conference on Unmanned Aircraft Systems, which he runs annually. Dr. Valavanis was a Distinguished Speaker in the IEEE Robotics and Automation Society, a Senior Member of IEEE, a Fellow of the American Association for the Advancement of Science, a Fellow of the U.K. Institute of Measurement and Control, and a Technical Expert of the NATO Science and Technology Organization (STO). He was also selected to serve as NATO Technical Evaluator for the AVT-353 Workshop on 'Artificial Intelligence in the Cockpit for UAVs' that will take place in Torino, Italy, in April 2022. In August of 2021, he was also appointed to the NATO STO Technical Team of SAS-ET-EX on "Integration of Unmanned Systems into Operational Units" for the duration of the Program of Work. He is also a Fulbright Scholar (Senior Lecturing & Research Award).

Margareta Stefanovic Ph.D., received a Ph.D. in Electrical Engineering, Control Systems, from the University of Southern California. She is an Associate Professor at the University of Denver, Department of Electrical and Computer Engineering. Her research interests include robust adaptive control of uncertain systems, multiagent systems and distributed control. She serves as Subject Editor for the International Journal of Robust and Nonlinear Control, Editorat-Large for Journal of Intelligent and Robotic Systems, and Associate Editor of ISA Transactions. She is a Senior Member of the Institute of Electrical and Electronics Engineers (IEEE). Dr. Stefanovic is co-author of the book "Safe Adaptive Control: Data-driven Stability Analysis and Robust Synthesis" (Lecture Notes in Control and Information Sciences, Springer).

Matthew J. Rutherford Ph.D., is an Associate Professor in the Department of Computer Science with a joint appointment in the Department of Electrical and Computer Engineering at the University of Denver. He is also Deputy Director of the DU Unmanned Systems Research Institute (DU²SRI). His research portfolio includes: the development of advanced controls and communication mechanisms for autonomous aerial and ground robots; applications of real-time computer vision to robotics problems using GPU-based parallel processing; testing and dynamic evaluation of embedded, real-time systems; development of complex mechatronic systems (mechanical, electrical, and software); the development of software techniques to reduce the amount of energy being consumed by hardware; development of a high-precision propulsion system for underwater robots.

Alessandro Rizzo Ph.D., received the Laurea degree (summa cum laude) in computer engineering and the Ph.D. degree in automation and electronics engineering from the University of Catania, Italy, in 1996 and 2000, respectively. In 1998, he has worked as a EURATOM Research Fellow with JET Joint Undertaking, Abingdon, U.K., researching on sensor validation and fault diagnosis for nuclear fusion experiments. In 2000 and 2001, he has worked as a Research Consultant at ST Microelectronics, Catania Site, Italy, and as an Industry Professor of robotics with the University of Messina, Italy. From 2002 to 2015, he was a tenured Assistant Professor with the Politecnico di Bari, Italy. In November 2015, he joined the Politecnico di Torino. Since 2012, he has been a Visiting Professor with the New York University Tandon School of Engineering, Brooklyn, NY, USA. He is currently an Associate Professor with the Department of Electronics and Telecommunications, Politecnico di Torino, Italy. He is engaged in conducting and supervising research on complex networks and systems, modeling and control of nonlinear systems, and cooperative robotics. He is the author of two books, two international patents, and more than 150 papers on international journals and conference proceedings. He has been a recipient of the Award for the Best Application Paper at the IFAC world triennial conference in 2002 and of the Award for the Most Read Papers in Mathematics and Computers in Simulation (Elsevier) in 2009. He is also a Distinguished Lecturer of the IEEE Nuclear and Plasma Science Society and one of the recipients of the 2019 Amazon Research Awards.